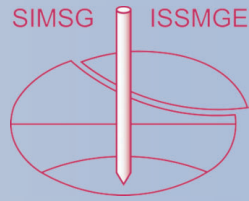
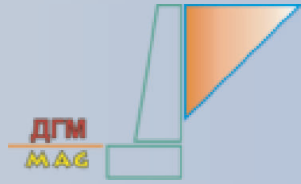


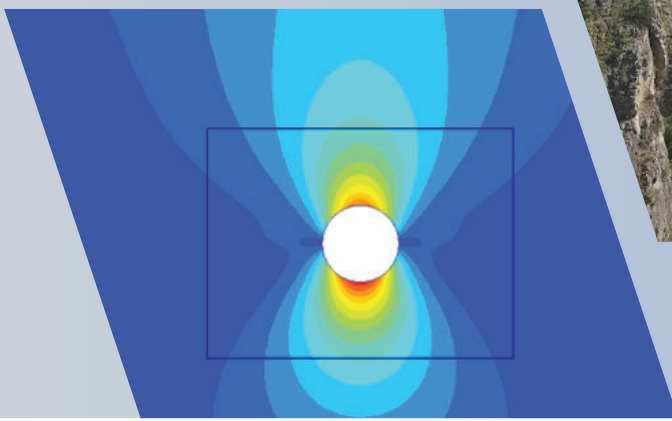
28TH

European Young Geotechnical Engineers Conference



EYGE 2024

Demir Kapija,
Macedonia



June 25 - June 29
2024

Proceedings of the 28th European Young Geotechnical
Engineers Conference – EYGEC 2024
Demir Kapija, R. N. Macedonia

Editor

Igor Peševski

President of the Macedonian Association for Geotechnics

Proceedings of the 28th European Young Geotechnical Engineers Conference – EYGEC 2024

Издавач:

Друштво за геотехника на Македонија, седиште Партизански одреди бр.24, 1000 Скопје.

Илустратор: Тамара Јовановска

Компјутерска подготовка: Ангела Маринковска

Тираж: 100 примероци

The 28th European Young Geotechnical Engineers Conference – EYGEC 2024 is organized by the Macedonian Association for Geotechnics (MAG), with the support of the International Society for Soil Mechanics and Geotechnical Engineering (ISSMGE). The conference was held in Demir Kapija, R.N. Macedonia in period 25-29.06.2024

© 2024 Macedonian Association for Geotechnics, Skopje, R.N. Macedonia

All rights reserved. No part of this publication or the information contained herein may be reproduced, stored in a retrieval system, or transmitted in any form or by means, electronic, mechanical, by photocopying, recording otherwise, without written prior permission from the publishers.

Published by: Macedonian Association for Geotechnics

Copies 100

ISBN: 978-608-4510-61-1

COMPARISON DESIGN-MONITORING A DIAPHRAGM WALL FOR A DEEP EXCAVATION UP TO 11.60M.....	77
Ciumeică Daniel	
1915 ÇANAKKALE BRIDGE EUROPEAN ANCHOR BLOCK EXCAVATION PROJECT: A CASE STUDY	85
Ahmet Dinc, Alp Gokalp, Senol Adatepe	
IMPROVING AXIAL PILE DESIGN THROUGH FULL-SCALE FIELD TESTING AND FIBRE OPTIC SENSING.....	94
Kevin J. Duffy	
CASE STUDY ON THE NUMERICAL MODELLING OF A CFA ENERGY PILE..	100
Ugur Can Erginag, Semra Polat, Mert Guner, Melis Sutman, Ozer Cinicioglu	
PARAMETER OPTIMIZATION FOR CONSTITUTIVE SOIL MODELS USING SUPERVISED MACHINE LEARNING	106
Haris Felić, Islam Marzouk, Franz Tschuchnigg	
WATER RETENTION CHARACTERISTICS AND DRAINED SHEAR STRENGTH OF SOIL TREATED WITH NEWLY DEVELOPED SOIL CONDITIONERS	115
Barbara Fortuna, Alessandro Sorze, Francesco Valentini, Jasna Smolar	
KINEMATIC EFFECTS ON INTERACTION DIAGRAMS FOR CAISSON FOUNDATIONS	123
Domenico Gaudio, Cristian Passeri, Sebastiano Rampello	
AUTOMATED SIMPLE TELL-TALE DEVICE FOR DETECTING LOSS OF BACKFILL SOIL THROUGH JOINTS OF QUAYS.....	129
Carlos Laina-Gómez, Enrique Asanza-Izquierdo	
DIRECT AND ALTERNATIVE METHODS FOR DETERMINING THE MAXIMUM SHEAR MODULUS (G_0) OF SOILS	135
Kristina Ilieva	
GEOTECHNICAL MODELLING OF ROCK MASS - HYDROTECHNICAL STRUCTURES INTERACTION	143
Tamara Jovanovska	
SHEAR MODULUS REDUCTION AND MATERIAL DAMPING CURVES MEASURED WITH RESONANT COLUMN DEVICE ON COHESIVE SOILS FROM THE LJUBLJANA MARSH	150
Timotej Jurček, Boštjan Pulko, Matej Maček	
ADVANTAGES OF 3D FEM MODELLING AND BIM MODELLING FOR UNDERGROUND STRUCTURES	159
Kristóf Kelemen	

Kinematic effects on Interaction Diagrams for Caisson Foundations

Domenico Gaudio^a, Cristian Passeri^b, Sebastiano Rampello^c

^a Sapienza University of Rome, Department of Structural and Geotechnical Engineering, via Eudossiana 18, 00184, Rome, Italy

ABSTRACT

Caisson foundations are typically designed against combined loading since they are usually adopted for long-span bridges and viaducts. Their capacity can be usefully expressed in terms of Interaction Diagrams (IDs), which represent the *locus* of the generalised forces ($N-Q-M$) bringing the soil-caisson system to limit conditions. Caisson IDs have been recently proposed for static conditions only, meaning that the limit generalised forces were computed assuming no inertial forces acting within the foundation soils. However, it is worth investigating whether these inertial forces may bring to a reduction of the system resistance, what is usually referred to as *kinematic effect*.

In this paper, the *kinematic effects* on the IDs for caisson foundations are assessed from the results of a parametric study, where 3D Finite Element pushover analyses were performed. A pseudo-static approach was followed, which implies that the inertial forces within the soil deposit were proportional to the self-weight of the soil via the seismic coefficient, k_h , which was assumed as constant and uniform over the calculation. The parametric study involved different caisson slenderness ratios, H/D , and initial loading factors, χ , the latter representing the degree of mobilisation of the soil-caisson strength against vertical loading before the earthquake: nonetheless, here only the results obtained with the values $H/D = 1$ and $\chi = 0.21$ are discussed, for the sake of space.

An analytical formulation of the IDs taking *kinematic effects* into account is finally provided, which may be adopted in the seismic design of caisson foundations.

KEYWORDS

Caisson foundation; Interaction Diagram; Kinematic effects; Pseudo-Static approach.

1. INTRODUCTION

Massive and rigid onshore caisson foundations are becoming increasingly popular over the years, due to the increasing span length of bridges and viaducts. Under these circumstances, loading conditions are becoming increasingly challenging indeed, due to the increase of inclination and eccentricity of loads acting atop the foundation. At the same time, safety requirements are getting stricter, particularly in the seismic design of Critical Infrastructures (CIs), which may be attributed to the higher level of performance needed to ensure their operation during and after the occurrence of destructive earthquakes.

From the foregoing it follows that the bearing capacity of soil-caisson systems is to be estimated carefully. Therefore, their resistance has increasingly been evaluated via Interaction Diagrams (IDs), which represent the *locus* of the generalised forces ($N-Q-M$) bringing the soil-caisson system to limit conditions. In seismic-prone areas, the detrimental effect of the inertial forces acting within the soil deposit, usually referred to as *kinematic effects*, should be considered in the design of caisson foundations. However, caisson IDs have only been proposed for static conditions so far (Gerolymos *et al.*, 2015; Zafeirakos and Gerolymos, 2016; Rosati *et al.*, 2023).

In this paper, the *kinematic effects* on caisson IDs are first evaluated from the results of 3D pushover analyses performed with the Finite Element (FE) method. In the analyses, a pseudo-static approach was followed to simulate the inertial forces acting within the soil deposit. The results obtained for a slenderness ratio $H/D = 1$ and an initial loading factor $\chi = 0.21$ are only discussed in this paper, for the sake of space, despite additional values were also considered in the parametric study, such as $H/D = 0.5$ and 2 and $\chi = 0, 0.42$. An analytical formulation of the IDs taking *kinematic effects* into account is finally given.

2. PROBLEM LAYOUT

The problem layout is given in Fig. 1: a caisson with a diameter D equal to its height H ($= 12$ m, $H/D = 1$), is embedded in a 5-m-thick gravelly sand layer over a 55-m-thick, slightly overconsolidated, silty clay stratum. The water table is located at the sand-clay contact and the pore pressure regime is hydrostatic. The Load Reference Point (LRP) was assumed at the caisson centroid, whereto the generalised forces N - Q - M , and displacements w , u and θ , are referred hereafter.

Fig. 1 also shows the profiles adopted in the Finite Element (FE) analyses both for the OverConsolidation Ratio, OCR , and the small-strain shear modulus, G_0 , the latter calibrated against the theoretical profile proposed by Hardin and Richart (1963) for the gravelly sand layer (relative density $D_R = 60\%$) and Rampello *et al.* (1995) for the silty clay (plasticity index $PI = 25\%$). The mechanical parameters adopted in the analyses are given in Tab. 1, where γ is the unit weight, ν is the Poisson ratio, c' and ϕ' are the effective cohesion and internal friction angle, and ψ is the dilatancy angle.

Table 1. Soil mechanical parameters

soil	γ (kN/m ³)	ν (-)	c' (kPa)	ϕ' (°)	ψ
sand	20	0.2	0	30	0
clay	20	0.2	20	23	0

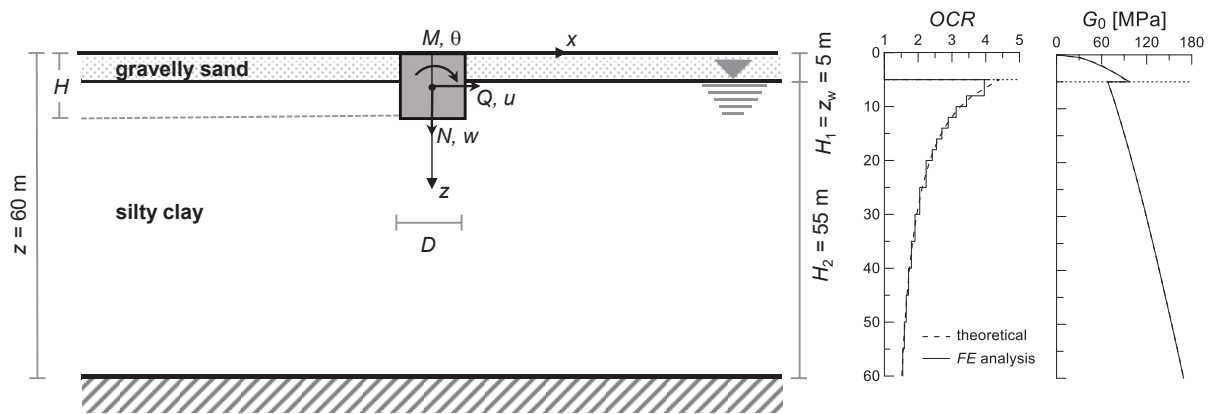


Figure 1. Problem layout

3. 3D FINITE ELEMENT MODELLING

The 3D FE mesh in Fig. 2 consists of 95500 10-node tetrahedral elements with 4 Gauss points (Bentley, 2021); this numerical domain was adopted to perform the pushover (*i.e.*, static nonlinear) analyses bringing the soil-caisson systems to limit conditions, as detailed below. Since the generalised forces applied to the caisson belong to the x - z plane, only half of the domain was considered. The bottom of the numerical model was fixed both against horizontal and vertical displacements ($u_x = u_y = u_z = 0$), whereas the horizontal displacements only were fixed along the vertical boundaries (either $u_x = 0$ or $u_y = 0$); the ground surface was left free to move. Preliminary analyses ensured that the presence of the outer boundaries did not alter the response of the soil-caisson systems (Gaudio *et al.*, 2024).

The clay stratum was subdivided into fifteen sublayers to reproduce the analytical profiles of *OCR*, which provided the stepwise profile plotted in Fig. 1. The mechanical soil behaviour was described with the *Hardening Soil with Small-Strain stiffness* model (*HSsmall*; Benz *et al.*, 2009) and a Mohr-Coulomb failure criterion (Tab. 2).

Table 2. *HSsmall* parameters

soil	G_0^{ref} (MPa)	m (-)	$\gamma_{0.7}$ (%)	$E'_{\text{ur}}{}^{\text{ref}}$ (MPa)	ν_{ur} (-)	$E'_{50}{}^{\text{ref}}$ (MPa)	$E'_{\text{oad}}{}^{\text{ref}}$ (MPa)
sand	145.7	0.61	0.024	174.9	0.2	58.3	58.3
clay	65.7	0.75	0.045	58.2	0.2	19.4	19.4

The mechanical behaviour of the caisson foundation was simulated with a non-porous elastic material, characterised by the concrete Young modulus, $E_c = 30$ GPa, and a Poisson ratio $\nu_c = 0.15$, while its weight was reproduced via a vertical force applied atop the caisson rather than with imposing the unit weight, in order not to induce any pseudo-static force into the caisson. Purely attritive interface elements were assigned to the soil-caisson contact to simulate any relative sliding, with a reduced friction angle, $\delta = \tan^{-1}[2/3 \cdot \tan\phi]$.

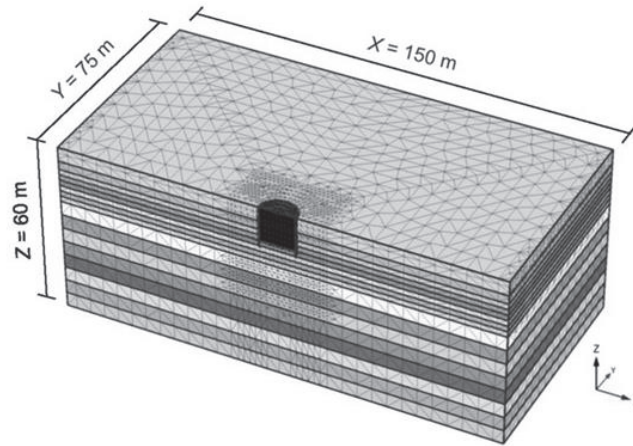


Figure 2. 3D FE model adopted in the parametric study

In the parametric study, the wished-in-place caisson was first subjected, in drained conditions, to a vertical load N . The value of N was determined to provide specific values of the initial loading factor, here defined as the inverse of the static safety factor under vertical loading only, $\chi = 1/F_{\text{sv}}$. Then, the entire numerical domain which had been previously assigned a unit weight (*i.e.*, the soil deposit) was subjected to a field of uniform horizontal body forces, proportional to the pseudo-static coefficient k_h ; in this phase, undrained conditions were adopted, to mimic what typically observed during seismic shaking for soil deposits such as the one at hand. Finally, a horizontal force Q and a moment M were applied to the caisson until limit conditions were reached, by keeping the pseudo-static coefficient k_h on. The generalised loads were applied with a ratio $\alpha_G = M_G/Q_G$, where the subscript G indicates that the generalised forces were referred to the caisson centroid (LRP).

The ID obtained for the specific case $H/D = 1$, $\chi = 0.21$, and $k_h = -0.2$, is plotted in Fig. 3a (sign convention for k_h is also provided in the Figure). The ID was computed considering two distinct criteria to detect the ultimate conditions of the soil-caisson system, such as the proper triggering of bearing capacity under inclined and eccentric loading conditions (*plateau* in the legend) and the attainment of a global stiffness K equal to 1% of the unstressed, initial stiffness, K_0 , as first proposed by Zafeirakos and Gerolymos (2016). Both criteria are defined based on the non-dimensional pushover curve $\bar{F}-\bar{u}$, where \bar{F} and \bar{u} are:

$$\bar{F} = \sqrt{\xi^2 + \mu^2}; \bar{u} = \sqrt{\left(\frac{u_G}{D}\right)^2 + \theta^2} \quad (1)$$

where ξ and μ are the non-dimensional horizontal force and moment, respectively, defined as

$$\xi = \frac{Q}{N_{lim,net}}; \mu = \frac{M}{D \cdot N_{lim,net}} \quad (2)$$

with $N_{lim,net}$ being the limit vertical load computed in drained conditions, while u_G and θ are the caisson horizontal displacement and rotation at the caisson centroid, respectively.

The pushover curve obtained for the specific value $\alpha_G = -6$ m is plotted in Fig. 3b, whose *plateau* is reached for excessive caisson displacements. Hence, the ultimate conditions along this pushover curve were detected imposing the criterion $K/K_0 = 1\%$, where $K = \Delta\bar{F}/\Delta\bar{u}$. The remarkable outcome stemming from the comparison of the IDs computed with the two criteria is that they are homothetic, which implies that the tangent criterion can be adopted as a displacement-based criterion for detecting ultimate conditions for caisson foundations.

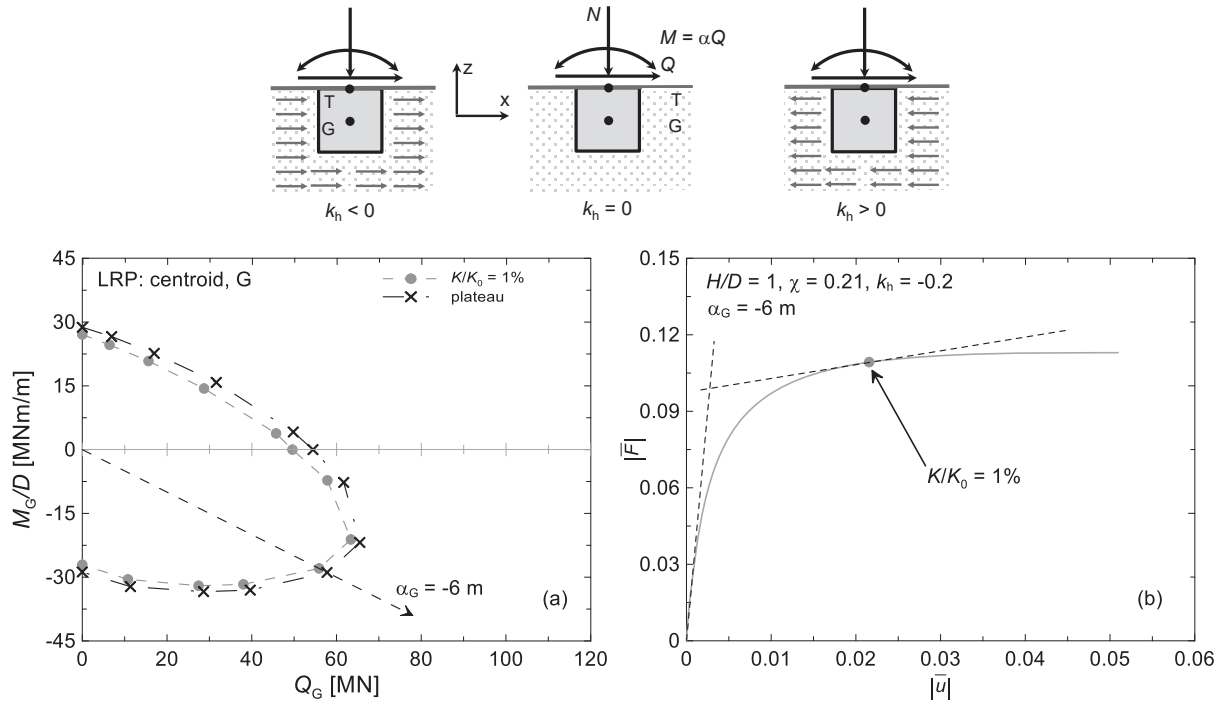


Figure 3. (a) ID from different criteria; (b) dimensionless pushover curve obtained for $\alpha_G = -6$ m

4. KINEMATIC EFFECTS

The kinematic effects obtained for the specific case of a caisson with $H/D = 1$ subjected to an initial loading factor $\chi = 0.21$ are represented in Fig. 4, for all values of the horizontal seismic coefficient k_h considered in the parametric study ($0, \pm 0.10, \pm 0.15$, and ± 0.20), representative of a small-to-medium intensity seismic events. The IDs are plotted through dimensional (Fig. 4a) and non-dimensional (Fig. 4b) representations, where the former exhibits the influence of k_h on the ID size, whereas the latter reveals the role of kinematic effects on the ID shape (Q_u and M_u represent the limit values of Q and M when the other component is null: $Q_u = Q_{(M=0)}$ and $M_u = M_{(Q=0)}$).

It is apparent that the ID size (Fig. 4a) is influenced by the seismic coefficient k_h , with an ID shrinkage for $k_h < 0$, which can be ascribed to the soil inertial forces acting along the same direction as Q . Indeed, these forces add to the load already coming from the superstructure, whereas the opposite is observed for $k_h > 0$, where the inertial forces counteract Q . This holds true particularly in the fourth quadrant, where the overstrength of the soil-caisson system is exhibited, whereas the limit overturning moment is almost insensitive to k_h . Similarly, the ID shape turned out not to be affected by the kinematic effects

(Fig. 4b), which would strongly simplify the analytical derivation of caisson IDs for seismic conditions, as shown in the following.

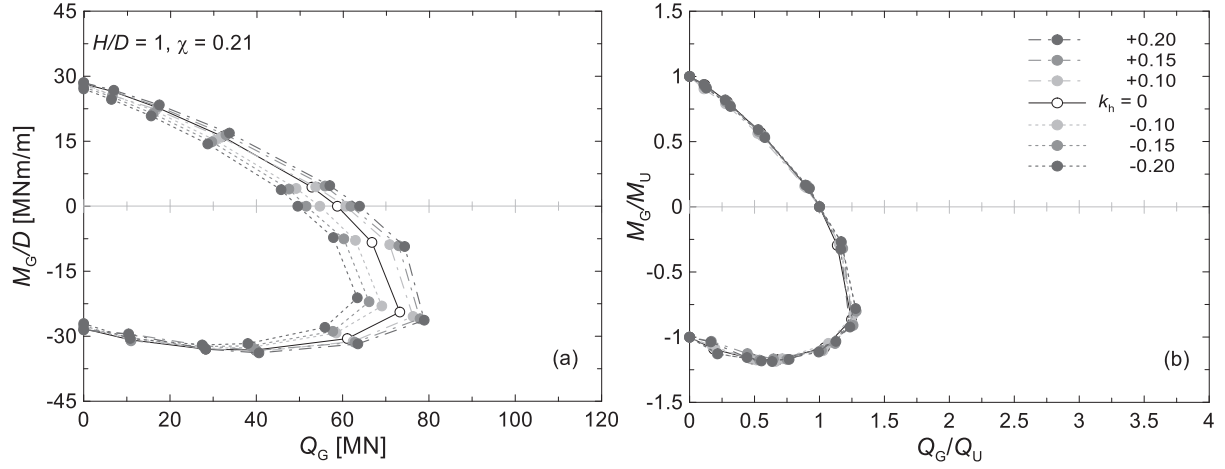


Figure 4. Kinematic effects on the ID: (a) size; (b) shape ($H/D = 1$, $\chi = 0.21$)

5. ANALYTICAL RELATIONSHIPS FOR IDS ACCOUNTING FOR THE KINEMATIC EFFECTS

The numerical results were fitted in the non-dimensional space χ - ξ - μ by adopting the following implicit functional form to describe the 3D surface, after Butterfield and Gottardi (1994):

$$\left(\frac{\cos^2 \omega}{a_\xi^2} + \frac{\sin^2 \omega}{a_\mu^2} \right) \xi^2 + \left(\frac{\sin^2 \omega}{a_\xi^2} + \frac{\cos^2 \omega}{a_\mu^2} \right) \mu^2 + \sin 2\omega \left(\frac{1}{a_\xi^2} - \frac{1}{a_\mu^2} \right) \xi\mu = 1 \quad (3)$$

where a_ξ and a_μ are the semi-axes of the ellipse in the ξ - μ plane and ω is its counterclockwise angle of inclination measured starting from the ξ axis. These geometrical parameters express the 3D surface enclosing the dependency of both the ID size and shape on the slenderness ratio, H/D , the initial loading factor, χ , and the horizontal seismic coefficient, k_h . For the sake of brevity, the relevant functional forms are not reported here, but the values attained for the specific cases under consideration are reported instead ($H/D = 1$, $\chi = 0.21$), namely $a_\xi = 0.142$, $a_\mu = 0.047$ and $\omega = -15.082^\circ$ for $k_h = +0.2$ and $a_\xi = 0.110$, $a_\mu = 0.045$, and $\omega = -19.518^\circ$ for $k_h = -0.2$. The comparison between the FE and the analytical ID is given in Fig. 5, where the static ID ($k_h = 0$) is also plotted: the ID expansion and shrinkage with respect to the static conditions is well reproduced. More details on this are discussed in Gaudio *et al.* (2024).

6. CONCLUDING REMARKS

In this paper, IDs for caisson foundations were computed from an extensive parametric study where 3D FE pushover analyses were conducted in undrained conditions, until limit conditions were attained for the soil-caisson system. In the analyses, the inertia forces developing into the soil deposit during seismic shakings were simulated following a pseudo-static approach, thus being proportional to the unit weight of the soil through the seismic coefficient k_h . A general, displacement-based criterion to detect the limit load was adopted, which consisted in a reduction of the global soil-caisson stiffness up to 1% of the unstressed one. The results of the parametric study clearly showed that kinematic effects may significantly alter the ID size with respect to the reference static conditions ($k_h = 0$), making the ID expand or shrink, while almost keeping the static ID shape. Analytical equations were finally proposed for a preliminary design of caisson foundations under seismic shaking, enclosing kinematic effects.

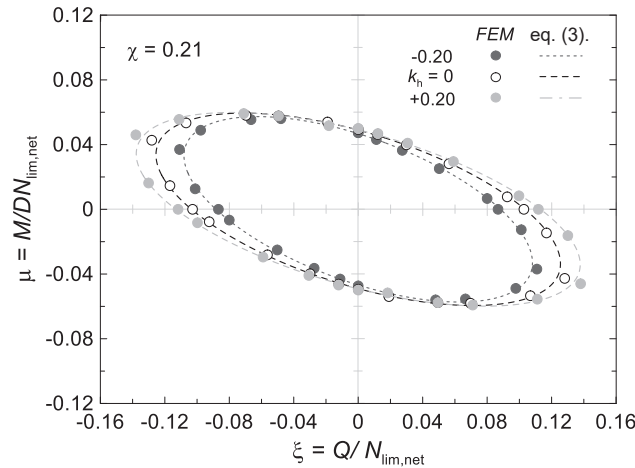


Figure 5. FE and analytical IDs computed for $H/D=1$, $\chi = 0.21$, and $k_h = 0, \pm 0.2$

7. ACKNOWLEDGEMENTS

The Authors would like to express their sincere gratitude to Prof. Claudio di Prisco for his useful comments and suggestions. The help provided by Dr. Alessandra Rosati is also acknowledged.

REFERENCES

- Bentley. 2021. *Plaxis 3D CE Reference Manuals*.
- Benz, T., Vermeer, P. A. and Schwab, R. 2009. A small-strain overlay model. *Int. J. Numer. Anal. Meth. Geomech.*, 33(1), 25–44.
- Butterfield, R. and Gottardi, G. 1994. A complete three-dimensional failure envelope for shallow footings on sand. *Géotechnique*, 44(1), 181-184.
- Gaudio, D., Passeri, C. and Rampello, S. 2024. Interaction domains for caisson foundations under seismic loading. *Computers & Geotechnics (submitted for evaluation)*
- Gerolymos, N., Zafeirakos, A. and Karapiperis, K. 2015 Generalized failure envelope for caisson foundations in cohesive soil: Static and dynamic loading. *Soil Dyn. Earthq. Eng.*, 78, 154-174.
- Hardin, B. O., Richart, F. E. 1963. Elastic wave velocities in granular soils. *J. Soil. Mech. Found. Div.*, 89, 33-65.
- Rampello, S., Viggiani, G. M. B. and Silvestri, F. 1995. The dependence of G_0 on stress state and history in cohesive soils. In: *Shibuya S et al. (ed) Pre-Failure Deformation Characteristics of Geomaterials – Measurements and application*. Balkema A.A., Rotterdam, Brookfield, Sapporo, vol 2, pp 1155-1160.
- Rosati, A., Gaudio, D., di Prisco, C. G., Rampello, S. 2023. Use of interaction domains for a displacement-based design of caisson foundations. *Acta Geotechnica*, 18(1), 445-468. DOI: 10.1007/s11440-022-01547-z
- Zafeirakos, A. and Gerolymos, N. 2016. Bearing strength surface for bridge caisson foundations in frictional soil under combined loading. *Acta Geotechnica*, 11(5), 1189-1208.

28TH
European Young Geotechnical Engineers Conference

